Journal of Superconductivity: Incorporating Novel Magnetism, Vol. 17, No. 5, October 2004 (© 2004)

Pancake Vortices

John R. Clem[1]

Received August 15, 2004; accepted September 4, 2004

I describe the magnetic-field and current-density distributions generated by two-dimensional (2D) pancake vortices in infinite, semi-infinite, and finite-thickness stacks of Josephson-decoupled superconducting layers. Arrays of such vortices have been used to model the magnetic structure in highly anisotropic layered cuprate high-temperature superconductors. I show how the electromagnetic forces between pancake vortices can be calculatated, and I briefly discuss the effects of interlayer Josephson coupling.

KEY WORDS: pancake vortices; layered superconductors; high-temperature superconductors; films; forces; Josephson coupling.

1. INTRODUCTION

Since this paper is intended for publication in a special Festschrift issue honoring Mike Tinkham, I have been invited to include some personal reflections in the introduction. I believe I first heard his name when I was a graduate student in the early 1960s at the University of Illinois-Urbana, working on extensions of the BCS theory [1] to include anisotropy of the superconducting energy gap [2,3]. A paper by Ginsberg, Richards, and Tinkham [4] had reported results on the far-infrared absorption in superconducting lead, which showed a precursor hump in the real part of the complex conductivity, $\sigma_1(\omega)/\sigma_N$. I tried to explain this feature in terms of gap anisotropy but was unsuccessful.

Throughout subsequent years, I have followed Mike Tinkham's career with considerable interest. I have admired his research style, which consistently has resulted in new and interesting experimental results and theoretical interpretations that advance the theory. I also admire anyone who can write carefully prepared books, and I have found his books on superconductivity (in both editions [5,6]) to be particularly useful. I have asked students beginning research with me to work diligently through these books to learn the fundamentals of superconductivity.

One of the topics that Mike Tinkham finds interesting is vortex physics, and since this has been one of my main research interests, I would like to focus here on one aspect: two-dimensional (2D) pancake vortices. This is a favorite subtopic of mine, partly because I coined the name and partly because my 1991 paper on this subject [7] has been so well received by the superconductivity community (over 600 citations to date). Incidentally, although I wanted to put "2D pancake vortex" in the title of this paper, the editors of *Physical Review B* forbid this but did allow me to use these words in the abstract and the rest of the paper. I first reported on my work on 2D pancake vortices at a Gordon Research Conference chaired by Mike Tinkham in June 1989, but (as has too often been the case with me) I was slow to publish, and some of the key results were published in 1990 by Artemenko and Kruglov [8] and by Buzdin and Feinberg [9]. I later discovered that the basic solution had even been published in 1979 by Efetov [10], but his work unfortunately had gone largely unnoticed.

This paper is organized as follows. In Sec. 2, I calculate the properties of 2D pancake vortices in an infinite stack of Josephson-decoupled superconducting layers, first by considering all the layers as being very thin and then by considering the layers above and below the pancake layer as a continuum [11]. In Sec. 3, I use the continuum approach to calculate the properties of 2D pancake vortices in a semi-infinite stack of Josephson-decoupled superconducting

[1]Ames Laboratory and Department of Physics and Astronomy, Iowa State University, Ames, Iowa 50011-3160.

layers. In Sec. 4, I again use the continuum approach to calculate the properties of 2D pancake vortices in a finite stack of Josephson-decoupled superconducting layers [12], first for arbitrary thickness and then for a thickness much less than the in-plane penetration depth, where the results bear some similarities to those of Pearl [13–15] for vortices in thin films. In Sec. 5, I show how to calculate the electromagnetic forces between pancake vortices, and in Sec. 6, I discuss some consequences of Josephson coupling. I conclude with a brief summary in Sec. 7.

2. PANCAKE VORTEX IN AN INFINITE STACK OF SUPERCONDUCTING LAYERS

The chief motivation for my work that led to the idea of the 2D pancake vortex was the question of how to describe the vortex structure of highly anisotropic layered cuprate high-temperature superconductors, with Bi-2212 ($Bi_2Sr_2CaCu_2O_{8-\delta}$) being the best-known example. Applying the anisotropic Ginzburg-Landau equations [16–29] to this material, it could easily be seen that the calculated value of the coherence length ξ_c (the length scale describing spatial variation of the order parameter in the c direction perpendicular to the layers) was less than the center-to-center distance s between the CuO_2 bilayers. Since the Ginzburg-Landau theory assumes that all the characteristic lengths of superconductivity are large by comparison with atomic length scales, this fact indicated that some other theory was needed to describe details of the vortex structure in the most anisotropic high-T_c superconductors.

The natural way to incorporate the existence of discrete layers was to make use of the Lawrence-Doniach theory [30], which treats the intralayer behavior using Ginzburg-Landau theory but interlayer coupling via the Josephson effect [31]. In this theory the coherence length ξ_c plays no role when its value is less than s, and the penetration depth λ_c describing the length scale of the spatial variation of supercurrents parallel to the c direction can be related to the maximum Josephson supercurrent J_0 via [32] $\lambda_c = (c\phi_0/8\pi^2 s J_0)^{1/2}$ in Gaussian units. The parameter usually used to characterize the degree of anisotropy is $\gamma = \lambda_c/\lambda_{ab}$, where λ_{ab} is the penetration depth describing the length scale of the spatial variation of supercurrents parallel to the layers (neglecting the anisotropy between the a and b directions, i.e., assuming for simplicity that $\lambda_a \approx \lambda_b \approx \lambda_{ab}$). For Bi-2212, the value of γ is so large that it is difficult to measure [33]; γ was found in Ref. [34] to be larger than 150, but a more recent quantitative determination [35] has yielded $\gamma = 640 \pm 25$.

For such highly anisotropic materials, it seemed sensible to me to take the limit $\gamma \to \infty$ ($\lambda_c = \infty$ or $J_0 = 0$) as the starting point to describe vortex structure. The essential idea was that in a model of identical superconducting layers separated by insulating layers, one could solve for the magnetic field and current density generated by a 2D pancake vortex in one of the superconducting layers when the other layers contained no vortices but served only to screen the magnetic field generated by the pancake vortex. With this solution as a building block, one could then find the magnetic field produced by a stack of such pancake vortices, even if misaligned, by the process of linear superposition. This was basically the approach I had used in developing the theory that quantitatively explains the coupling forces between misaligned vortices in just two layers [36,37], the primary and secondary superconducting layers of the dc transformer studied experimentally first by Giaever [38,39], and later by Solomon [40], Sherrill [41], Deltour and Tinkham [42], and Cladis *et al.* [43,44], but in greatest detail by Ekin *et al.* [45,46].

2.1. Model of Very Thin Discrete Superconducting Layers

To calculate the magnetic-field and current-density distributions generated by a pancake vortex in an infinite stack of Josephson-decoupled superconducting layers, in Ref. [7] I used the model in which the superconducting layers, all of thickness d, are centered on the planes $z = z_n = ns$ ($n = 0, \pm1, \pm2, \ldots$), as sketched in Fig. 1. The London penetration depth within each layer is λ_s such that the average penetration depth for currents parallel to the layers is [32] $\lambda_\parallel = \lambda_s(s/d)^{1/2}$, which corresponds to the penetration depth λ_{ab} in the high-temperature superconductors. When the central layer ($z = 0$) contains a vortex at the origin but all other layers are vortex-free, the London fluxoid quantization condition [47] in layer n can be expressed as

$$2\pi\rho[a_\phi(\rho, z_n) + (2\pi\Lambda_s/c)K_\phi(\rho, z_n)] = \phi_0\delta_{n0}, \quad (1)$$

where in cylindrical coordinates $\boldsymbol{a}(\rho, z) = \hat{\phi}a_\phi(\rho, z)$ is the vector potential, $\boldsymbol{K}(\rho, z_n) = \hat{\phi}K_\phi(\rho, z_n) = \hat{\phi}\bar{j}_\phi(\rho, z_n)$s is the sheet-current density in layer n averaged over the periodicity length s, $\Lambda_s = 2\lambda_\parallel^2/s = 2\lambda_s^2/d$ is the 2D screening length, and $\phi_0 = hc/2e$

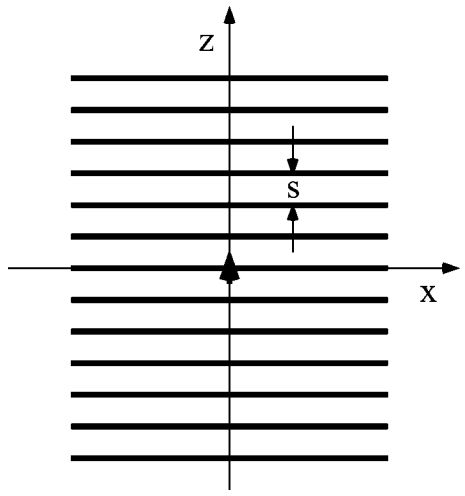

Fig. 1. Infinite stack of thin superconducting layers with a pancake vortex at the origin (bold arrow).

is the superconducting flux quantum. Equation (1) inevitably leads to a description of vortices in the London model [48], which is characterized by unphysical current-density and magnetic-field singularities on the vortex axis. The pioneering work on vortices by Abrikosov [49] showed that such singularities are cut off at a distance of the order of the in-plane coherence length ξ_{ab}. A simple model for the vortex core, employing a variational core-radius parameter $\xi_v \sim \xi_{ab}$, has been used to describe straight vortices in isotropic [50] and anisotropic [51] superconductors, as well as in films of arbitrary thickness, whether isolated [52] or in superconducting dc transformers [37]. This model also could be used to cure the vortex-core singularities that are present in all the following results of this paper.

If one takes the thickness d of each layer to be very small, as in Ref. [7], the vector potential can be expressed in the form

$$a_\phi(\rho, z) = \int_0^\infty dq A(q) J_1(q\rho) Z(q, z), \tag{2}$$

where $J_1(q\rho)$ is a Bessel function and $Z(q, z)$ has scallops as a function of z that are necessary to describe the discontinuities of $b_\rho(\rho, z)$ arising from the induced sheet currents $K_\phi(\rho, z_n)$ for $n \neq 0$. Note that $\boldsymbol{b}(\rho, z) = \nabla \times \boldsymbol{a}(\rho, z)$, such that

$$b_\rho(\rho, z) = -\frac{\partial a_\phi(\rho, z)}{\partial z} \tag{3}$$

and

$$b_z(\rho, z) = \frac{1}{\rho} \frac{\partial[\rho a_\phi(\rho, z)]}{\partial \rho}. \tag{4}$$

Inserting the exact expression for $A(q)$ into Eq. (2) yields a complicated integral that cannot be integrated analytically. However, a close approximation to the exact result can be obtained by writing $Z(q, z) = \exp(-Q|z|)$, where $Q = (q^2 + \lambda_\parallel^{-2})^{1/2}$ and $A(q) = \phi_0/2\pi\Lambda_s Q$; this approximation, which is valid for $s \ll \lambda_\parallel$, corresponds to retaining information on the scale of $\lambda_\parallel$ but giving up detailed information on the finer scale of s. The resulting vector potential and magnetic field components are

$$a_\phi(\rho, z) = \frac{\phi_0 \lambda_\parallel}{2\pi\Lambda_s \rho}(e^{-|z|/\lambda_\parallel} - e^{-r/\lambda_\parallel}), \tag{5}$$

$$b_z(\rho, z) = \frac{\phi_0}{2\pi\Lambda_s r} e^{-r/\lambda_\parallel}, \tag{6}$$

$$b_\rho(\rho, z) = \frac{\phi_0}{2\pi\Lambda_s \rho}\left[\frac{z}{|z|} e^{-|z|/\lambda_\parallel} - \frac{z}{r} e^{-r/\lambda_\parallel}\right], \tag{7}$$

where $r = (\rho^2 + z^2)^{1/2}$. Since in the high-temperature superconductors $s/2\lambda_\parallel = \lambda_\parallel/\Lambda_s \approx 10^{-2}$, the vector potential term in Eq. (1) of order $\lambda_\parallel/\Lambda_s$ can be neglected in the central layer ($n = 0$) and we obtain to good approximation

$$K_\phi(\rho, z_0) = \frac{c\phi_0}{4\pi^2 \Lambda_s \rho}. \tag{8}$$

However, for all the other layers ($n \neq 0$) we obtain

$$K_\phi(\rho, z_n) = -\frac{c\phi_0 \lambda_\parallel}{4\pi^2 \Lambda_s^2 \rho}(e^{-|z_n|/\lambda_\parallel} - e^{-r_n/\lambda_\parallel}), \tag{9}$$

where $z_n = ns$ and $r_n = (\rho^2 + z_n^2)^{1/2}$. Note that the magnitude of the sheet-current density in the $n = 0$ central layer is much larger, by a factor of order 10^2, than the sheet-current density in one of the $n \neq 0$ layers. It is for this reason that I gave the name pancake vortex to this field and current distribution.

An interesting property of the above solutions is that the pancake-vortex-generated magnetic flux $\Phi_z(\rho, z) = 2\pi\rho a_\phi(\rho, z)$ up through a circle of radius ρ at height z is (using $\Lambda_s = 2\lambda_\parallel^2/s$)

$$\Phi_z(\rho, z) = \phi_0(s/2\lambda_\parallel)(e^{-|z|/\lambda_\parallel} - e^{-r/\lambda_\parallel}), \tag{10}$$

such that the magnetic flux up through a layer at height z is

$$\Phi_z(\infty, z) = \phi_0(s/2\lambda_\parallel)e^{-|z|/\lambda_\parallel}, \tag{11}$$

and the magnetic flux up through the central layer at $z = 0$ is

$$\Phi_z(\infty, 0) = \phi_0(s/2\lambda_\parallel). \tag{12}$$

When $s \ll \lambda_\parallel$, as in the high-temperature superconductors, we see that $\Phi_z(\infty, 0) \ll \phi_0$. This is at first

surprising until one realizes that fluxoids are quantized in superconductors but flux is not [47]. In the present problem, the fluxoid is the quantity on the left-hand side of Eq. (1), and since $(2\pi\Lambda_s/c)K_\phi(\rho, z_0)$ is proportional to $1/\rho$ and $a_\phi(\rho, z_0)$ is very small, the fluxoid is due almost entirely to the current term. Note also that $\Phi_z(\infty, \infty) = 0$; this occurs because all the magnetic flux up through the central layer $z = 0$ is directed radially outward by the screening currents in the layers with $z > 0$.

On the other hand, an infinite stack of pancake vortices, whether straight or not, has quite different magnetic-flux properties. If there is one pancake vortex in every layer at $z = z_n = ns\,(n = 0, \pm1, \pm2, \ldots)$, then the magnetic flux up through the central layer (and by symmetry any other layer) is

$$\Phi_z(\infty, 0) = \phi_0(s/2\lambda_\parallel) \sum_{n=-\infty}^{\infty} e^{-|z_n|/\lambda_\parallel} = \phi_0, \qquad (13)$$

where the last equality is obtained by evaluating the sum and making use of the property that $s \ll \lambda_\parallel$. Similarly, the radial magnetic field at $\rho = \infty$ and $z = 0$ is now zero, since the positive contributions from all the pancake vortices below the central layer are canceled by the negative contributions from the pancake vortices above this layer.

2.2. Continuum Model

The solutions given in Eqs. (5)–(9) can be obtained more easily by regarding the $n \neq 0$ layers as a continuum, characterized by the penetration depth $\lambda_\parallel$ for currents parallel to the layers [11]. Moreover, for a realistic treatment of stacks of just a few superconducting layers, a model accounting for finite layer thickness s is needed. We therefore use the model sketched in Fig. 2 and write the London equation [47] in cylindrical coordinates in the form

$$2\pi\rho[a_\phi(\rho, z) + (4\pi\lambda_\parallel^2/c)j_\phi(\rho, z)] = \phi_0\delta_{n0}, \qquad (14)$$

where the delta function on the right-hand side accounts for the presence of a vortex aligned along the z axis in the $n = 0$ layer ($|z| < s/2$). Combining this equation with Ampere's law, $j_\phi = (c/4\pi)(\partial b_\rho/\partial z - \partial b_z/\partial\rho)$, and making use of Eqs. (3) and (4), we obtain the partial differential equation

$$\frac{\partial^2 a_\phi}{\partial z^2} + \frac{\partial^2 a_\phi}{\partial\rho^2} + \frac{1}{\rho}\frac{\partial a_\phi}{\partial\rho} - \left(\frac{1}{\rho^2} + \frac{1}{\lambda_\parallel^2}\right) a_\phi = -\frac{\phi_0}{2\pi\lambda_\parallel^2\rho}\,\delta_{n0}, \qquad (15)$$

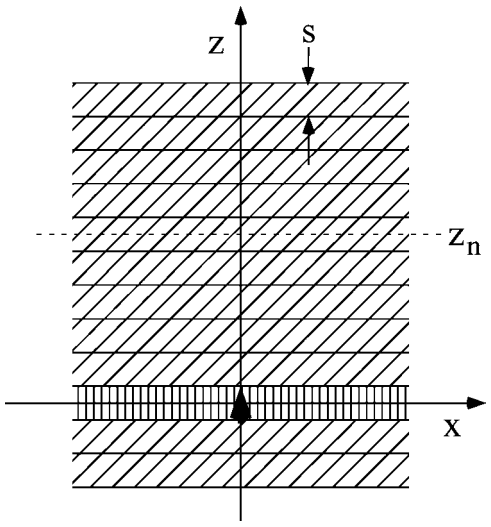

Fig. 2. Continuum model of an infinite stack of superconducting layers with a pancake vortex (bold arrow at the origin) in the layer at $z = z_0 = 0$.

which can be solved by writing $a_\phi(\rho, z)$ in the three regions $z > s/2$, $-s/2 < z < s/2$, and $z < -s/2$ in terms of Hankel components [53] as follows:

$$a_\phi(\rho, z) = \int_0^\infty dq A_a(q) J_1(q\rho) e^{-Qz}, \quad z \geq s/2, \qquad (16)$$

$$a_\phi(\rho, z) = \int_0^\infty dq \left[\frac{\phi_0}{2\pi\lambda_\parallel^2 Q^2} + A_{0-}(q)e^{-Qz} + A_{0+}(q)e^{Qz}\right] J_1(q\rho), \quad -s/2 \leq z \leq s/2, \qquad (17)$$

$$a_\phi(\rho, z) = \int_0^\infty dq A_b(q) J_1(q\rho) e^{-z}, \quad z \leq -s/2, \qquad (18)$$

where $Q = (q^2 + 1/\lambda_\parallel^2)^{1/2}$. The four unknown functions $A_a(q), A_{0-}(q), A_{0+}(q)$, and $A_b(q)$ can be obtained by applying the boundary conditions of continuity of $a_\phi(\rho, z)$ and $b_\rho(\rho, z)$ [Eq. (3)] at the two interfaces $z = \pm s/2$, carrying out the Hankel transforms using [54]

$$\int_0^\infty d\rho\rho J_1(q\rho) J_1(q'\rho) = (1/q)\delta(q - q'), \qquad (19)$$

and solving the four resulting linear equations. The results are

$$A_{0-}(q) = A_{0+}(q) = -\frac{\phi_0}{4\pi\lambda_\parallel^2 Q^2}\, e^{-Qs/2}, \qquad (20)$$

$$A_a(q) = A_b(q) = \frac{\phi_0 \sinh(Qs/2)}{2\pi\lambda_\parallel^2 Q^2}. \quad (21)$$

Note that $s \ll \lambda_\parallel$, such that if we confine our attention to values of $\rho \gg s$, the integrals in Eqs. (16)–(18) are dominated by values of $q \ll 1/s$. We then may make the replacement $\sinh(Qs/2) \to Qs/2$, which makes $A_a = A_b = \phi_0/2\pi\Lambda_s Q$, the same as $A(q)$ in Ref. [7] and Sec. 2.1.

The magnetic flux up through a circle of radius ρ in the plane with coordinate z is $\Phi_z(\rho, z) = 2\pi\rho a_\phi(\rho, z)$. Evaluating the integrals for $a_\phi(\rho, z)$ [Eqs. (16)–(18)] in the limit $\rho \to \infty$, we can show without making the approximation that $s \ll \lambda_\parallel$ that the pancake-vortex-generated magnetic flux through a layer at height z, where $|z| > s/2$, is

$$\Phi_z(\infty, z) = \phi_0 \sinh(s/2\lambda_\parallel) e^{-|z|/\lambda_\parallel}, \quad (22)$$

and the total magnetic flux up through the central layer at $z = 0$ is

$$\Phi_z(\infty, 0) = \phi_0(1 - e^{-s/2\lambda_\parallel}) \approx \phi_0(s/2\lambda_\parallel). \quad (23)$$

If there is one pancake vortex in every layer at $z = z_n = ns\,(n = 0, \pm1, \pm, 2, \ldots)$, even if they are misaligned, then by summing the contributions given in Eqs. (22) and (23) we find that the magnetic flux up through the central layer (and by symmetry any other layer) is exactly ϕ_0. If all the vortices are aligned along the z axis, the magnetic-field and current-density distributions reduce to those of the London model [48], for which

$$a_\phi(\rho) = \frac{\Phi_z(\rho)}{2\pi\rho} = \frac{\phi_0}{2\pi\rho}\left[1 - \frac{\rho}{\lambda_\parallel} K_1\left(\frac{\rho}{\lambda_\parallel}\right)\right], \quad (24)$$

$$b_z(\rho) = \frac{\phi_0}{2\pi\lambda_\parallel^2} K_0\left(\frac{\rho}{\lambda_\parallel}\right), \quad (25)$$

$$j_\phi(\rho) = \frac{c\phi_0}{8\pi\lambda_\parallel^3} K_1\left(\frac{\rho}{\lambda_\parallel}\right), \quad (26)$$

and $b_\rho(\rho) = 0$, where $K_n(x)$ is a modified Bessel function.

3. PANCAKE VORTEX IN A SEMI-INFINITE STACK OF SUPERCONDUCTING LAYERS

In Sec. 2, I reviewed the results found in Ref. [7] for a pancake vortex in an infinite stack of superconducting layers, where it is seen that the fields and currents decay exponentially on the scale of $\lambda_\parallel$ above and below the layer containing the pancake vortex. For a sample of thickness $D \gg \lambda_\parallel$ it is therefore clear that the fields and currents generated by pancake vortices that are many $\lambda_\parallel$ from either surface are essentially the same as in Sec. 2. However, the fields and currents are significantly altered when a pancake vortex is less than $\lambda_\parallel$ from the surface of a sample of thickness $D \gg \lambda_\parallel$ or when the sample thickness D is comparable with or smaller than $\lambda_\parallel$. In this section I use the continuum approximation described in Sec. 2.2 to obtain solutions describing the field and currents generated by a vortex in an arbitrary layer of a semi-infinite stack of superconducting layers. In the next section (Sec. 4) I present solutions for a pancake vortex in a finite stack of arbitrary thickness D.

Consider a semi-infinite stack of superconducting layers, with the top surface on the xy plane, such that all the layers are in the region $z < 0$, as sketched in Fig 3. We number the superconducting layers such that the layer $n = 0$ in the region $z_{0-} < z < z_{0+}$, centered at $z = z_0 < 0$, is the one containing the pancake vortex. The other layers are centered at $z = z_n = z_0 + ns$, where positive (negative) n labels layers above (below) the pancake vortex. If there are N_+ layers above the pancake vortex, then the top layer is centered at $z = z_0 + N_+ s = D/2 - s/2$. By so numbering the layers, we still can use Eq. (14) as the London fluxoid quantization condition.

As in Sec. 2, we may write the vector potential in cylindrical coordinates as $a(\rho, z) = \hat{\phi} a_\phi(\rho, z)$. However, we now have different expressions for $a_\phi(\rho, z)$

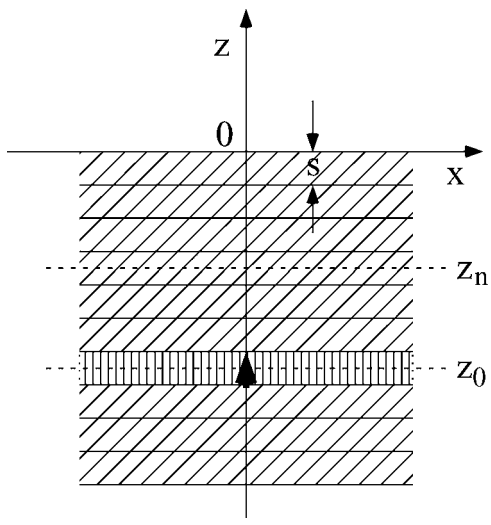

Fig. 3. Continuum model of a semi-infinite stack of superconducting layers in the space $z < 0$ with a pancake vortex (bold arrow) in the layer at $z = z_0$.

in four regions:

$$a_\phi(\rho, z) = \int_0^\infty dq A_>(q) J_1(q\rho) e^{-qz}, \quad z \geq 0, \tag{27}$$

$$a_\phi(\rho, z) = \int_0^\infty dq \left[A_{a-}(q) e^{-Q(z-z_0)} + A_{a+}(q) e^{Q(z-z_o)} \right] \times J_1(q\rho), \quad z_{0+} \leq z \leq 0, \tag{28}$$

$$a_\phi(\rho, z) = \int_0^\infty dq \left[\frac{\Phi_0}{2\pi\lambda_\parallel^2 Q^2} + A_{0-}(q) e^{-Q(z-z_o)} + A_{0+}(q) e^{Q(z-z_0)} \right] J_1(q\rho), \quad z_{0-} \leq z \leq z_{0+}, \tag{29}$$

$$a_\phi(\rho, z) = \int_0^\infty dq A_b(q) J_1(q\rho) e^{Q(z-z_0)}, \quad z \leq z_{0-}, \tag{30}$$

where $Q = (q^2 + \lambda_\parallel^{-2})^{1/2}$ and $z_{0\pm} = z_0 \pm s/2$. The six functions $A_>(q)$, $A_{a-}(q)$, $A_{a+}(q)$, $A_{0-}(q)$, $A_{0+}(q)$, and $A_b(q)$, obtained by applying the six boundary conditions of continuity of $a_\phi(\rho, z)$ and $b_\rho(\rho, z)$ [calculated from Eq. (3)] at $z = 0$, z_{0+}, and z_{0-}, are

$$A_>(q) = \frac{\phi_0 \sinh(Qs/2)}{\pi\lambda_\parallel^2 Q^2 (1 + q/Q)} e^{Qz_0}, \tag{31}$$

$$A_{a-}(q) = \frac{\phi_0 \sinh(Qs/2)}{2\pi\lambda_\parallel^2 Q^2}, \tag{32}$$

$$A_{a+}(q) = \frac{\phi_0 \sinh(Qs/2)}{2\pi\lambda_\parallel^2 Q^2} \left(\frac{1 - q/Q}{1 + q/Q} \right) e^{2Qz_0}, \tag{33}$$

$$A_{0-}(q) = -\frac{\phi_0}{4\pi\lambda_\parallel^2 Q^2} e^{-Qs/2}, \tag{34}$$

$$A_{0+}(q) = -\frac{\phi_0}{4\pi\lambda_\parallel^2 Q^2} \left[e^{-Qs/2} - 2\sinh(Qs/2) \times \left(\frac{1 - q/Q}{1 + q/Q} \right) e^{2Qz_0} \right], \tag{35}$$

$$A_b(q) = \frac{\phi_0 \sinh(Qs/2)}{2\pi\lambda_\parallel^2 Q^2} \left[1 + \left(\frac{1 - q/Q}{1 + q/Q} \right) e^{2Qz_0} \right]. \tag{36}$$

Although the resulting integrals for $a_\phi(\rho, z)$ and those [via Eqs. (3) and (4)] for $b_\rho(\rho, z)$ and $b_z(\rho, z)$ can easily be calculated numerically, they are too complicated to evaluate analytically for arbitrary ρ and z. On the other hand, we can evaluate them approximately for large ρ. When $\rho \gg \lambda_\parallel$, the values of q that dominate the integrals in Eqs. (27)–(30) via the Bessel function $J_1(q\rho)$ are those of order $1/\rho \ll 1/\lambda_\parallel$, such that we may replace all quantities under the integral except $J_1(q\rho)$ by their values at $q = 0$. Similarly, because of the factor $\exp(-qz)$ in Eq. (16) we may replace $A_>(q)$ by $A_>(0)$ to evaluate $a_\phi(\rho, z)$ when ρ is small but $z \gg \lambda_\parallel$.

The magnetic flux up through a circle of radius ρ in the plane with coordinate z is $\Phi_z(\rho, z) = 2\pi\rho a_\phi(\rho, z)$. Evaluating the integrals as indicated above for $a_\phi(\rho, z)$ in the limit as $\rho \to \infty$, we obtain for the total magnetic flux up through the plane with coordinate z:

$$\Phi_z(\infty, z) = 2\phi_0 \sinh(s/2\lambda_\parallel) e^{z_0/\lambda_\parallel}, \quad z \geq 0, \tag{37}$$

$$\Phi_z(\infty, z) = 2\phi_0 \sinh(s/2\lambda_\parallel) \cosh(z/\lambda_\parallel) e^{z_0/\lambda_\parallel}, \quad z_{0+} \leq z \leq 0, \tag{38}$$

$$\Phi_z(\infty, z) = \phi_0 \{ 1 - \cosh[(z - z_0)/\lambda_\parallel] e^{-s/2\lambda_\parallel} + \sinh(s/2\lambda_\parallel) e^{(z+z_0)/\lambda_\parallel} \}, \quad z_{0-} \leq z \leq z_{0+}, \tag{39}$$

$$\Phi_z(\infty, z) = 2\phi_0 \sinh(s/2\lambda_\parallel) \times \cosh(z_0/\lambda_\parallel) e^{z/\lambda_\parallel}, \quad z \leq z_{0-}. \tag{40}$$

When the pancake vortex is in the top layer (i.e., when $z_0 = -s/2$), the magnetic flux $\Phi_z(\infty, 0)$ up through the top surface is approximately $\phi_0(s/\lambda_\parallel)$, since $s/\lambda_\parallel \sim 10^{-2} \ll 1$. When the pancake vortex is in a layer much farther than $\lambda_\parallel$ from the top surface, the amount of magnetic flux up through the top surface $\Phi_z(\infty, 0)$ [Eq. (37)] becomes exponentially small (recall that $z_0 < 0$). The precise magnetic field distribution generated in the space above the superconductor within $\lambda_\parallel$ of the origin can be calculated numerically for a given pancake-vortex position z_0 from Eqs. (3), (4), and (27). However, at distances $r = \sqrt{\rho^2 + z^2}$ somewhat larger than $\lambda_\parallel$ from the origin, we have to good approximation for $z \geq 0$.

$$a_\phi(\rho, z) = \frac{\Phi_z(\infty, 0)}{2\pi\rho} \left(1 - \frac{z}{r} \right), \tag{41}$$

$$b_\rho(\rho, z) = \frac{\Phi_z(\infty, 0)}{2\pi} \frac{\rho}{r^3}, \tag{42}$$

$$b_z(\rho, z) = \frac{\Phi_z(\infty, 0)}{2\pi} \frac{z}{r^3}. \tag{43}$$

In other words, the magnetic field generated by the pancake vortex appears as if generated by a magnetic monopole, with the flux $\Phi_z(\infty, 0)$ [Eq. (37)] spreading out evenly into the hemisphere above the surface. It is important to note that only pancake vortices

within about $\lambda_\parallel$ (or λ_{ab} in the high-temperature superconductors) are visible using Bitter decoration, scanning Hall-probe microscopy, scanning SQUID microscopy, or magneto-optical techniques; pancake vortices deeper than this make an exponentially small contribution to the magnetic field above the surface.

From Eq. (39) we see that the magnetic flux up through the plane $z = z_0$ in the layer containing the pancake vortex is

$$\Phi_z(\infty, z_0) = \phi_0[1 - e^{-s/2\lambda_\parallel} + \sinh(s/2\lambda_\parallel)e^{2z_0/\lambda_\parallel}] \approx \phi_0(s/2\lambda_\parallel)(1 + e^{2z_0/\lambda_\parallel}). \quad (44)$$

When the pancake vortex is in the top layer (i.e., if $z_0 = -s/2$), the magnetic flux up through this layer is approximately $\phi_0(s/\lambda_\parallel)$, and when the pancake vortex is deep inside the superconductor (i.e., if $-z_0 \gg \lambda_\parallel$), the magnetic flux up through the pancake layer is approximately $\phi_0(s/2\lambda_\parallel)$, as found in Sec. 2 for the infinite superconductor [Eqs. (12) and (23)].

If there is a pancake vortex in every layer, even if they are misaligned, the total magnetic flux up through any plane with coordinate z is exactly equal to ϕ_0. This can be shown by replacing z_0 by $z_n = z_0 + ns$, noting that the top layer is centered at $-s/2$, and summing over all n, using Eq. (37) if $z > 0$. On the other hand, if $z < 0$, one must use Eq. (40) for the top layers for which $z_n - s/2 \geq z$, Eq. (39) for the layer containing z for which $z_n - s/2 \leq z \leq z_n + s/2$, and Eq. (38) for the remaining layers for which $z_n + s/2 \leq z$. If all the pancake vortices are aligned along the z axis, the magnetic-field and current-density distributions reduce to those calculated by Pearl [11,53,55] for a vortex in a semi-infinite superconductor.

Scanning Hall-probe experiments visualizing vortices in underdoped, highly anisotropic $YBa_2Cu_3O_{6+x}$ (YBCO) single crystals, where $x = 0.35 - 0.375$, recently have been carried out by Guikema [56]. In the most underdoped crystals, the observations revealed what at first appeared to be "partial vortices" carrying magnetic flux less than ϕ_0. Guikema concluded, however, that such images are caused by a full vortex that is partially displaced horizontally, i.e., a "split pancake-vortex stack." The magnetic flux generated above the surface by the two parts of the vortex stack can be calculated as follows. Suppose the bottom portion, consisting of pancake vortices below the plane $z = -d$, is aligned along the z axis, and the top portion, consisting of pancake vortices above the plane $z = -d$, is aligned parallel to the z axis but at $(x, y) = (x_0, 0)$. Using Eq. (37) to sum the contributions from the pancake vortices in the two portions, one finds that the magnetic flux $\Phi_{\text{bot}} = \phi_0 \exp(-d/\lambda_\parallel)$ generated by the bottom portion emerges from the vicinity of the origin $(x, y, z) = (0, 0, 0)$, and the magnetic flux $\Phi_{\text{top}} = \phi_0[1 - \exp(-d/\lambda_\parallel)]$ generated by the top portion emerges from the vicinity of the point $(x, y, z) = (x_0, 0, 0)$. The two flux contributions should be resolvable when the displacement x_0 exceeds the Hall-probe size and the probe's field sensitivity allows detection of both contributions.

4. PANCAKE VORTEX IN A FINITE STACK OF SUPERCONDUCTING LAYERS

Since all laboratory samples of the high-temperature superconductors are of finite thickness, it is important to examine how the properties of pancake vortices discussed in Sec. 2 are modified when we take the finite thickness into account, including the possibility that the thickness D may be less than the penetration $\lambda_\parallel$. Let us begin by considering a pancake vortex centered on the z axis in a stack of superconducting layers, each of thickness s, in the region $-D/2 < z < D/2$, as sketched in Fig. 4. As in the previous section, we number the layers such that the layer $n = 0$ at $z = z_0$, where $|z_0| \leq (D/2 - s/2)$, is the one containing the pancake vortex. The other layers are centered at $z = z_n = z_0 + ns$, where positive (negative) n labels layers above (below) the pancake vortex. If there are N_+ layers above the

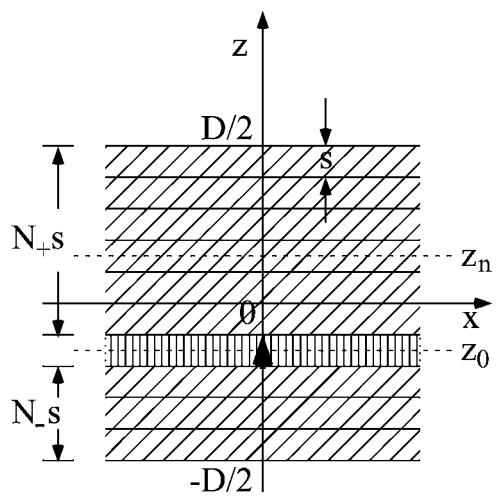

Fig. 4. Continuum model of a stack of superconducting layers in the space $|z| < D/2$ with a pancake vortex (bold arrow) in the layer at $z = z_0$.

pancake vortex, then the top layer is centered at $z = z_0 + N_+ s = D/2 - s/2$, and if there are N_- layers below the pancake vortex, then the bottom layer is centered at $z = z_0 - N_- s = -D/2 + s/2$. As in Sec. 2.2, I treat all the layers using the continuum approximation and use Eq. (14) as the London fluxoid quantization condition. In Sec. 4.1, I show how to calculate the fields generated by a pancake vortex in a finite stack of Josephson-decoupled superconducting layers, each of thickness s, with an arbitrary total stack thickness D relative to $\lambda_\parallel$. In Sec. 4.2, I consider the simplifications that arise when $D \ll \lambda_\parallel$, which corresponds to the case of high-temperature superconducting samples consisting of roughly 10 or fewer unit cells along the c direction.

4.1. Finite Stack of Arbitrary Thickness

As in Secs. 2.2 and 3, we write the vector potential in cylindrical coordinates as $\mathbf{a}(\rho, z) = \hat{\phi} a_\phi(\rho, z)$. However, we now have different expressions for $a_\phi(\rho, z)$ in five regions:

$$a_\phi(\rho, z) = \int_0^\infty dq A_>(q) J_1(q\rho) e^{-q(z-D/2)}, \quad z \geq D/2, \tag{45}$$

$$a_\phi(\rho, z) = \int_0^\infty dq [A_{a-}(q) e^{-Q(z-D/2)} + A_{a+}(q) e^{Q(z-D/2)}] J_1(q\rho), \quad z_{0+} \leq z \leq D/2, \tag{46}$$

$$a_\phi(\rho, z) = \int_0^\infty dq \left[\frac{\phi_0}{2\pi\lambda_\parallel^2 Q^2} + A_{0-}(q) e^{-Q(z-z_0)} + A_{0+}(q) e^{Q(z-z_0)} \right] J_1(q\rho), \quad z_{0-} \leq z \leq z_{0+}, \tag{47}$$

$$a_\phi(\rho, z) = \int_0^\infty dq [A_{b-}(q) e^{-Q(z+D/2)} + A_{b+}(q) e^{Q(z+D/2)}] J_1(q\rho), \quad -D/2 \leq z \leq z_{0-}, \tag{48}$$

$$a_\phi(\rho, z) = \int_0^\infty dq A_<(q) J_1(q\rho) e^{q(z+D/2)}, \quad z \leq -D/2, \tag{49}$$

where $Q = (q^2 + \lambda_\parallel^{-2})^{1/2}$, the subscript a and (b) denotes the layered region above (below) the pancake vortex, and $z_{0\pm} = z_0 \pm s/2$. The eight functions $A_>(q), A_{a-}(q), A_{a+}(q), A_{0-}(q), A_{0+}(q), A_{b-}(q), A_{b+}(q)$, and $A_<(q)$, obtained by applying the eight boundary conditions of continuity of $a_\phi(\rho, z)$ and $b_\rho(\rho, z)$ [calculated from Eq. (3)] at $z = D/2$, z_{0-}, z_{0+}, and $-D/2$, are

$$A_>(q) = \frac{\phi_0}{\pi\lambda_\parallel^2 Q^2} \sinh(Qs/2) G(q, z_0), \tag{50}$$

$$A_{a-}(q) = \frac{\phi_0}{2\pi\lambda_\parallel^2 Q^2} \sinh(Qs/2)(1 + q/Q) G(q, z_0), \tag{51}$$

$$A_{a+}(q) = \frac{\phi_0}{2\pi\lambda_\parallel^2 Q^2} \sinh(Qs/2)(1 - q/Q) G(q, z_0), \tag{52}$$

$$\begin{aligned} A_{0-}(q) &= -\frac{\phi_0}{4\pi\lambda_\parallel^2 Q^2} [e^{Qs/2} - 2\sinh(Qs/2)(1 + q/Q) \times G(q, z_0) e^{QD/2} e^{-Qz_0}] \\ &= -\frac{\phi_0}{4\pi\lambda_\parallel^2 Q^2} [e^{-Qs/2} - 2\sinh(Qs/2)(1 - q/Q) \times G(q, -z_0) e^{-QD/2} e^{-Qz_0}], \end{aligned} \tag{53}$$

$$\begin{aligned} A_{0+}(q) &= -\frac{\phi_0}{4\pi\lambda_\parallel^2 Q^2} [e^{-Qs/2} - 2\sinh(Qs/2)(1 - q/Q) \times G(q, z_0) e^{-QD/2} e^{Qz_0}] \\ &= -\frac{\phi_0}{4\pi\lambda_\parallel^2 Q^2} [e^{Qs/2} - 2\sinh(Qs/2)(1 + q/Q) \times G(q, -z_0) e^{QD/2} e^{Qz_0}], \end{aligned} \tag{54}$$

$$A_{b-}(q) = \frac{\phi_0}{2\pi\lambda_\parallel^2 Q^2} \sinh(Qs/2)(1 - q/Q) G(q, -z_0), \tag{55}$$

$$A_{b+}(q) = \frac{\phi_0}{2\pi\lambda_\parallel^2 Q^2} \sinh(Qs/2)(1 + q/Q) G(q, -z_0), \tag{56}$$

$$A_<(q) = \frac{\phi_0}{\pi\lambda_\parallel^2 Q^2} \sinh(Qs/2) G(q, -z_0), \tag{57}$$

where

$$G(q, z) = \frac{(1 + q/Q) + (1 - q/Q) e^{-QD} e^{-2Qz}}{(1 + q/Q)^2 - (1 - q/Q)^2 e^{-2QD}} \times e^{-QD/2} e^{Qz}. \tag{58}$$

Although the resulting integrals for $a_\phi(\rho, z)$ and those [via Eqs. (3) and (4)] for $b_\rho(\rho, z)$ and $b_z(\rho, z)$ can easily be calculated numerically, they are too complicated to evaluate analytically for arbitrary ρ and z. On the other hand, we can evaluate them approximately for large ρ. When $\rho \gg \lambda_\parallel$, the values of q that dominate the integrals in Eqs. (45)–(49) via the Bessel function $J_1(q\rho)$ are those of order $1/\rho \ll 1/\lambda_\parallel$, such that we may replace all quantities under the integral except $J_1(q\rho)$ by their values at $q = 0$. Similarly, because of the factors $\exp(-qz)$ and $\exp(qz)$ in Eqs. (45) and (49) we may replace $A_>(q)$ by $A_>(0)$ and $A_<(q)$ by $A_<(0)$ to evaluate $a_\phi(\rho, z)$ when ρ is small but $|z| - D/2 \gg \lambda_\parallel$.

The magnetic flux up through a circle of radius ρ in the plane with coordinate z is $\Phi_z(\rho, z) = 2\pi\rho a_\phi(\rho, z)$. Evaluating the integrals as indicated above for $a_\phi(\rho, z)$ in the limit as $\rho \to \infty$, we obtain for the total magnetic flux up through the plane with coordinate z [12]:

$$\Phi_z(\infty, z) = 2\phi_0 \sinh\left(\frac{s}{2\lambda_\parallel}\right)\cosh\left(\frac{D/2 + z_0}{\lambda_\parallel}\right)/ \sinh\left(\frac{D}{\lambda_\parallel}\right), \quad z \geq D/2, \tag{59}$$

$$\Phi_z(\infty, z) = 2\phi_0 \sinh\left(\frac{s}{2\lambda_\parallel}\right)\cosh\left(\frac{D/2 + z_0}{\lambda_\parallel}\right) \times \cosh\left(\frac{D/2 - z}{\lambda_\parallel}\right)/\sinh\left(\frac{D}{\lambda_\parallel}\right), \quad z_{0+} \leq z \leq D/2, \tag{60}$$

$$\Phi_z(\infty, z) = \phi_0\left\{1 - \left[e^{(D-s)/2\lambda_\parallel}\cosh\left(\frac{D/2 - z_0}{\lambda_\parallel}\right) - e^{-(D-s)/2\lambda_\parallel}\cosh\left(\frac{D/2 + z_0}{\lambda_\parallel}\right)\right] \times e^{z/\lambda_\parallel}/2\sinh\left(\frac{D}{\lambda_\parallel}\right) - \left[e^{(D-s)/2\lambda_\parallel}\cosh\left(\frac{D/2 + z_0}{\lambda_\parallel}\right) - e^{-(D-s)/2\lambda_\parallel}\cosh\left(\frac{D/2 - z_0}{\lambda_\parallel}\right)\right] \times e^{-z/\lambda_\parallel}/2\sinh\left(\frac{D}{\lambda_\parallel}\right)\right\}, \quad z_{0-} \leq z \leq z_{0+}, \tag{61}$$

$$\Phi_z(\infty, z) = 2\phi_0 \sinh\left(\frac{s}{2\lambda_\parallel}\right)\cosh\left(\frac{D/2 - z_0}{\lambda_\parallel}\right) \times \cosh\left(\frac{D/2 + z}{\lambda_\parallel}\right)/\sinh\left(\frac{D}{\lambda_\parallel}\right), \quad -D/2 \leq z \leq z_{0-}, \tag{62}$$

$$\Phi_z(\infty, z) = 2\phi_0 \sinh\left(\frac{s}{2\lambda_\parallel}\right)\cosh\left(\frac{D/2 - z_0}{\lambda_\parallel}\right)/ \sinh\left(\frac{D}{\lambda_\parallel}\right), \quad z \leq -D/2. \tag{63}$$

The magnetic flux $\Phi_z(\infty, D/2)$ up through the top surface is given by Eq. (59). When $D \gg \lambda_\parallel$ and a pancake vortex is in the top layer (i.e., when $z_0 = D/2 - s/2$), we obtain $\Phi_z(\infty, D/2) \approx \phi_0(s/\lambda_\parallel)$, which is a tiny fraction of ϕ_0, since $s/\lambda_\parallel \sim 10^{-2} \ll 1$. As a function of the distance $D/2 - z_0$ of the pancake vortex from the top surface, we see that $\Phi_z(\infty, D/2) \approx \phi_0(s/\lambda_\parallel)\exp[-(D/2 - z_0)/\lambda_\parallel]$. When $D \ll \lambda_\parallel$, we find that $\Phi_z(\infty, D/2) \approx \phi_0(s/D) = \phi_0/N$, independent of the position z_0 of the pancake vortex within the stack, where $N = D/s$ is the number of layers in the sample. When $N = D/s = 1$, $\Phi_z(\infty, D/2) = \phi_0$, because our results then reduce to those of Pearl [13–15], who calculated the field and current distribution generated by a vortex in a film of thickness much less than the London penetration depth. The precise magnetic field distribution generated in the space above the superconductor can be calculated numerically for a given z_0 from Eqs. (3), (4), and (45). However, at distances $r_+ = \sqrt{\rho^2 + (z - D/2)^2}$ from the point on the surface directly above the pancake vortex that are larger than $\lambda_\parallel$ when $D > 2\lambda_\parallel$ or larger than the two-dimensional screening length $\Lambda_D = 2\lambda_\parallel^2/D$ when $D < 2\lambda_\parallel$, we have to good approximation for $z \geq D/2$

$$a_\phi(\rho, z) = \frac{\Phi_z(\infty, D/2)}{2\pi\rho}\left[1 - \frac{(z - D/2)}{r_+}\right], \tag{64}$$

$$b_\rho(\rho, z) = \frac{\Phi_z(\infty, D/2)}{2\pi}\frac{\rho}{r_+^3}, \tag{65}$$

$$b_z(\rho, z) = \frac{\Phi_z(\infty, D/2)}{2\pi}\frac{(z - D/2)}{r_+^3}. \tag{66}$$

In other words, the magnetic field generated by the pancake vortex appears as if generated by a positive magnetic monopole, with the flux $\Phi_z(\infty, D/2)$ [Eq. (59)] spreading out into the hemisphere above the surface.

Similar statements can be made about the magnetic flux $\Phi_z(\infty, -D/2)$ up through the bottom surface [Eq. (63)]. At large distances $r_- = \sqrt{\rho^2 + (z + D/2)^2}$ from the point on the surface directly below the pancake vortex, the magnetic field

appears as if generated by a negative magnetic monopole.

From Eq. (61), we see that the magnetic flux up through the plane $z = z_0$ in the layer containing the pancake vortex is

$$\Phi_z(\infty, z_0) = \phi_0 \left\{1 - \left[\sinh\left(\frac{D - s/2}{\lambda_\parallel}\right) - \sinh\left(\frac{s}{2\lambda_\parallel}\right) \times \cosh\left(\frac{2z_0}{\lambda_\parallel}\right)\right] / \sinh\left(\frac{D}{\lambda_\parallel}\right)\right\}. \quad (67)$$

When $D \gg \lambda_\parallel$, the dependence of this magnetic flux upon the distance $(D/2 - |z_0|)$ from the top or bottom surface is given by $\Phi_z(\infty, z_0) \approx \phi_0(s/2\lambda_\parallel)\{1 + \exp[-2(D/2 - |z_0|)/\lambda_\parallel]\}$. When the pancake vortex is in the top or bottom layer (i.e., if $|z_0| = D/2 - s/2$), the magnetic flux up through this layer is approximately $\phi_0(s/\lambda_\parallel)$, and when the pancake vortex is deep inside the superconductor (i.e., if $D/2 - |z_0| \gg \lambda_\parallel$), the magnetic flux up through the pancake layer is approximately $\phi_0(s/2\lambda_\parallel)$ as found in Sec. 2 for the infinite superconductor [Eqs. (12) and (23)]. When $D \ll \lambda_\parallel$, we see that $\Phi_z(\infty, z_0) \approx \phi_0(s/D) = \phi_0/N$, independent of the position z_0 of the pancake vortex within the stack, where $N = D/s$ is the number of layers in the sample.

If there is a pancake vortex in every layer, even if they are misaligned, the total magnetic flux up through any plane with coordinate z is exactly equal to ϕ_0. This can be shown by replacing z_0 by $z_n = z_0 + ns$ and summing over all n, using Eq. (59) if $z > D/2$ or Eq. (63) if $z < -D/2$. On the other hand, if $|z| < D/2$, one must use Eq. (62) for the top layers for which $z_n - s/2 \geq z$, Eq. (61) for the layer containing z for which $z_n - s/2 \leq z \leq z_n + s/2$, and Eq. (60) for the remaining layers for which $z_n + s/2 \leq z$. If all the vortices are aligned along the z axis, the magnetic-field and current-density distributions reduce to those given in Ref. [52] when $\xi_\nu = 0$.

It is possible that scanning Hall-probe or magneto-optical experiments may be able to detect partial vortices or split pancake-vortex stacks [56] carrying magnetic flux less than ϕ_0 in samples of highly anisotropic layered superconductors of thickness $D < \lambda_\parallel$. The magnetic flux generated above the surface $z = D/2$ by the two parts of the vortex stack can be calculated as follows. Suppose the bottom portion, consisting of pancake vortices below the plane $z = D/2 - d$, is aligned along the z axis, and the top portion, consisting of pancake vortices above the plane $z = D/2 - d$, is aligned parallel to the z axis but at $(x, y) = (x_0, 0)$. Using Eq. (59) to sum the contributions from the pancake vortices in the two portions, one finds that the magnetic flux $\Phi_{\text{bot}} = \phi_0 \sinh[(D - d)/\lambda_\parallel]/\sinh(D/\lambda_\parallel)$ generated by the bottom portion emerges from the vicinity of the point $(x, y, z) = (0, 0, D/2)$, and the magnetic flux $\Phi_{\text{top}} = \phi_0\{1 - \sinh[(D - d)/\lambda_\parallel]/\sinh(D/\lambda_\parallel)\}$ generated by the top portion emerges from the vicinity of the point $(x, y, z) = (x_0, 0, D/2)$, The two flux contributions should be resolvable when the displacement x_0 exceeds the Hall-probe size and the probe's field sensitivity allows detection of both contributions. Note that $\Phi_{\text{bot}} = \Phi_{\text{top}} = \phi_0/2$ when $d = D/2 \ll \lambda_\parallel$.

4.2. Finite Stack of Thickness $D \ll \lambda_\parallel$

Considerable simplifications occur when the thickness $D = Ns$ of the stack is much less than the in-plane penetration depth $\lambda_\parallel$ [11]. It is well known from the work of Refs. [13] and [14] that when $D \ll \lambda_\parallel$ the characteristic screening length in isolated films is not $\lambda_\parallel$ but rather the 2D screening length $\Lambda_D = 2\lambda_\parallel^2/D$. This is also true for the case of Josephson-decoupled stacks of total thickness D considered here. We may derive equations for $a_\phi(\rho, z)$, $b_\rho(\rho, z)$, and $b_z(\rho, z)$ valid for $D \ll \lambda_\parallel$ and $\rho \gg \lambda_\parallel$ by starting with Eqs. (45)–(49), applying Eqs. (3) and (4), and making the replacement $e^{\pm Qz} = \cosh(Qz) \pm \sinh(Qz)$. Since we are most interested in values of ρ of the order of Λ_D or larger, because of the presence of $J_1(q\rho)$ the dominant values of q in the resulting integrals are of the order of $q \sim 1/\Lambda_D \ll 1/\lambda_\parallel$, such that Q can be replaced by $1/\Lambda_\parallel$, and small quantities of the order of $D/\lambda_\parallel$ and $q\lambda_\parallel$ are of the same order of magnitude. Expanding in powers of the small quantities ($D/\lambda_\parallel$ and $q\lambda_\parallel$), we find that both $a_\phi(\rho, z)$ and $b_z(\rho, z)$ are to lowest order independent of z, with small correction terms of the order of $D/\lambda_\parallel$, such that to good approximation we may write these quantities as

$$a_\phi(\rho, z) = \frac{\phi_0}{2\pi N} \int_0^\infty dq \frac{J_1(q\rho)}{1 + q\Lambda_D} e^{-q(z - D/2)}, \quad z \geq D/2, \quad (68)$$

$$a_\phi(\rho, z) = \frac{\phi_0}{2\pi N} \int_0^\infty dq \frac{J_1(q\rho)}{1 + q\Lambda_D}, \quad -D/2 \leq z \leq D/2, \quad (69)$$

$$a_\phi(\rho, z) = \frac{\phi_0}{2\pi N} \int_0^\infty dq \frac{J_1(q\rho)}{1 + q\Lambda_D} e^{q(z + D/2)}, \quad z \leq -D/2, \quad (70)$$

$$b_z(\rho, z) = \frac{\phi_0}{2\pi N}\int_0^\infty dq \frac{qJ_0(q\rho)}{1+q\Lambda_D} e^{-q(z-D/2)}, \quad z \geq D/2, \tag{71}$$

$$b_z(\rho, z) = \frac{\phi_0}{2\pi N}\int_0^\infty dq \frac{qJ_0(q\rho)}{1+q\Lambda_D}, \quad -D/2 \leq z \leq D/2, \tag{72}$$

$$b_z(\rho, z) = \frac{\phi_0}{2\pi N}\int_0^\infty dq \frac{qJ_0(q\rho)}{1+q\Lambda_D} e^{q(z+D/2)}, \quad z \leq -D/2. \tag{73}$$

On the other hand, the radial component of the magnetic field varies strongly with z :

$$b_\rho(\rho, z) = \frac{\phi_0}{2\pi N}\int_0^\infty dq \frac{qJ_1(q\rho)}{1+q\Lambda_D} e^{-q(z-D/2)}, \quad z \geq D/2, \tag{74}$$

$$b_\rho(\rho, z) = \frac{\phi_0}{2\pi N}\int_0^\infty dq \frac{qJ_1(q\rho)}{1+q\Lambda_D}, \quad z = D/2, \tag{75}$$

$$b_\rho(\rho, z) = b_\rho(\rho, D/2) + \frac{(D/2-z)}{(D/2)}\frac{a_\phi(\rho)}{\Lambda_D}, \quad z_{0+} \leq z \leq D/2, \tag{76}$$

$$b_\rho(\rho, z) = b_\rho(\rho, D/2) + \frac{(D/2-z)}{(D/2)}\frac{a_\phi(\rho)}{\Lambda_D} - \frac{(z_{0+}-z)}{(D/2)}\frac{\phi_0}{2\pi\Lambda_D\rho}, \quad z_{0-} \leq z \leq z_{0+}, \tag{77}$$

$$b_\rho(\rho, z) = b_\rho(\rho, D/2) + \frac{(D/2-z)}{(D/2)}\frac{a_\phi(\rho)}{\Lambda_D} - \frac{s}{(D/2)}\frac{\phi_0}{2\pi\Lambda_D\rho}, \quad -D/2 \leq z \leq z_{0-}, \tag{78}$$

$$b_\rho(\rho, z) = b_\rho(\rho, D/2) - \frac{2}{\Lambda_D}\left[\frac{\phi_0}{2\pi N\rho} - a_\phi(\rho)\right] = b_\rho(\rho, -D/2), z = -D/2, \tag{79}$$

$$b_\rho(\rho, z) = -\frac{\phi_0}{2\pi N}\int_0^\infty dq \frac{qJ_1(q\rho)}{1+q\Lambda_D} e^{q(z+D/2)}, \quad \times z \leq -D/2, \tag{80}$$

where we use $a_\phi(\rho)$ to denote the vector potential in the region $|z| \leq D/2$, since $a_\phi(\rho, z)$ is very nearly independent of z. The sheet current $K_n(\rho) = K_\phi(\rho, z_n) = s j_\phi(\rho, z_n)$ in layer n can be obtained from either $j_\phi(\rho, z) = (c/4\pi)\partial b_\rho(\rho, z)/\partial z$ or the fluxoid quantization condition [Eq. (14)]:

$$K_n(\rho) = \frac{c}{2\pi\Lambda_s}\left[\frac{\phi_0}{2\pi\rho}\delta_{n0} - a_\phi(\rho)\right], \tag{81}$$

Table I. Results for One Pancake Vortex in a Stack of N Superconducting Layers of Total Thickness $D = N_s \ll \lambda_\parallel$ in the Limits $D \ll \rho \ll \Lambda_D = 2\lambda_\parallel^2/D$ and $\rho \gg \Lambda_D$ [Since D is very small, $r = (\rho^2 + z^2)^{1/2}$ may be regarded as the distance from the pancake vortex, and $|z|$ may be regarded as the distance from the top or bottom surface]

Physical quantity	$\rho \ll \Lambda_D$	$\rho \gg \Lambda_D$
$a_\phi(\rho, z)$	$\phi_0(r-\lvert z\rvert)/2\pi N\Lambda_D\rho$	$\phi_0(r-\lvert z\rvert)/2\pi N\rho r$
$a_\phi(\rho, 0)$	$\phi_0/2\pi N\Lambda_D$	$\phi_0/2\pi N\rho$
$\Phi_z(\rho, z) = 2\pi\rho a_\phi(\rho, z)$	$\phi_0(r-\lvert z\rvert)/N\Lambda_D$	$\Phi_0(r-\lvert z\rvert)/Nr$
$\Phi_z(\rho, z) = 2\pi\rho a_\phi(\rho, 0)$	$\phi_0\rho/N\Lambda_D$	ϕ_0/N
$b_\rho(\rho, z), z = \pm\lvert z\rvert$	$\pm\phi_0(r-\lvert z\rvert)/2\pi N\Lambda_D\rho r$	$\pm\phi_0\rho/2\pi Nr^3$
$b_\rho(\rho, \pm D/2)$	$\pm\phi_0/2\pi N\Lambda_D\rho$	$\pm\phi_0/2\pi N\rho^2$
$b_z(\rho, z)$	$\phi_0/2\pi N\Lambda_D r$	$\phi_0 z/2\pi Nr^3$
$b_z(\rho, 0)$	$\phi_0/2\pi N\Lambda_D\rho$	$\phi_0\lambda_D/2\pi N\rho^3$
$K_0(\rho) = K_\phi(\rho, z_0)$	$c\phi_0/4\pi^2 N\Lambda_D\rho$	$c\phi_0(N-1)/4\pi^2N^2\Lambda_D\rho$
$K_n(\rho) = K_\phi(\rho, z_n)$, $n \neq 0$	$-c\phi_0/4\pi^2N^2\Lambda_D^2$	$-c\phi_0/4\pi^2N^2\Lambda_D\rho$
$K_D(\rho)$	$c\phi_0/4\pi^2N\Lambda_D\rho$	$c\phi_0/4\pi^2N\rho^2$

where $\Lambda_s = 2\lambda_\parallel^2/s = N\Lambda_D$. The net sheet current through the thickness D is the sum of the K_n:

$$K_D(\rho) = \sum_{n=-N_-}^{N+} K_n(\rho) = \frac{c}{2\pi\Lambda_D}\left[\frac{\phi_0}{2\pi N\rho} - a_\phi(\rho)\right]. \tag{82}$$

The integrals appearing in Eqs. (68)–(82), which are evaluated in the Appendix, have simple forms in the limits $D \ll \rho \ll \Lambda_D$ and $\rho \gg \Lambda_D$. The corresponding expressions for the physical quantities we have calculated in this section are given in Table I. The magnetic-field and current-density distributions reduce to the thin-film results of Pearl [13,14] when $N = 1$ and $D = s$ or when each of the N layers contains a pancake vortex on the z axis.

5. FORCES

The force on a second pancake vortex at the position (ρ, z_n) due to a pancake vortex centered on the z axis at $(0, z_0)$ can be calculated from the Lorentz force [57]. Since pancake vortices cannot move out of their planes, the force is directed parallel to the planes in the radial $\hat{\rho}$ direction:

$$F_\rho(\rho) = K_\phi(\rho, z_n)\phi_0/c, \tag{83}$$

where

$$K_\phi(\rho, z_n) = \frac{c}{2\pi\Lambda_s}\left[\frac{\phi_0}{2\pi\rho}\delta_{n0} - a_\phi(\rho, z_n)\right] \tag{84}$$

is the sheet-current density and $a_\phi(\rho, z_n)$ is the vector potential at (ρ, z_n) generated by the pancake vortex at $(0, z_0)$, and $\Lambda_s = 2\lambda_\parallel^2/s = N\Lambda_D$.

If both pancake vortices are in the same plane, the interaction force is always repulsive and in an infinite or semi-infinite stack of superconducting layers is given to excellent approximation by

$$F_\rho(\rho) = \frac{\phi_0^2}{4\pi^2\Lambda_s\rho} \tag{85}$$

for all ρ. The reason for this is that the vector potential in Eq. (84) obeys $a_\phi(\rho, z_0) \le (s/\lambda_\parallel)(\phi_0/2\pi\rho) \ll \phi_0/2\pi\rho$, as shown in Secs. 2 and 3. However, for a finite stack of thickness $D \ll \lambda_\parallel$ consisting of N layers, Eq. (85) holds only for small ρ ($\rho \ll \Lambda_D$), where the vector potential in Eq. (84) is much smaller than $\phi_0/2\pi\rho$. As discussed in Sec. 4.1, the magnetic flux at infinite radius $\Phi_z(\infty, z_0)$ up through the pancake-vortex layer is approximately ϕ_0/N, which means that $a_\phi(\rho, z_0) \approx \phi_0/2\pi N\rho$ for large ρ, and

$$F_\rho(\rho) = \frac{(N-1)}{N}\frac{\phi_0^2}{4\pi^2\Lambda_s\rho}, \rho \gg \Lambda_D. \tag{86}$$

In the special case when $N = 2$, the repulsive force given in Eq. (86) is half that in Eq. (85).

If the two pancake vortices are in different planes, the $\phi_0/2\pi\rho$ term in Eq. (84) is absent, and the interaction force is given by

$$F_\rho(\rho) = -\frac{\phi_0 a_\phi(\rho, z_n)}{2\pi\Lambda_s}. \tag{87}$$

Because $a_\phi(\rho, z_n)$ is always positive, the interaction force is always negative, i.e., in a direction so as to cause the two pancake vortices to become aligned along the same vertical axis. For the general case, it is not a simple matter to calculate the spatial dependence of the attractive force between pancake vortices in different layers, as can be seen from the expressions for $a_\phi(\rho, z)$ given in previous sections. However, we can say that for an infinite or semi-infinite stack of superconducting layers, the magnitude of this attractive force is orders of magnitude smaller than the repulsive force between pancake vortices in the same layer. The attractive force between vortices in different layers in an infinite stack (or deep inside a semi-infinite stack) has a range $\lambda_\parallel$ in the z direction. Equation (5) shows that the attractive force in the infinite stack vanishes exponentially when the interplanar separation of the pancakes along the z direction exceeds $\lambda_\parallel$. For a finite stack of thickness $D = Ns \ll \lambda_\parallel$, we find that the attractive force between pancake vortices in different layers is

$$F_\rho(\rho) = -\frac{\phi_0^2}{4\pi^2\Lambda_s^2} = -\frac{\phi_0^2}{4\pi^2N^2\Lambda_D^2}, \quad D \ll \rho \ll \Lambda_D, \tag{88}$$

which agrees with the force in the infinite stack calculated from Eq. (9) when $|z_n| \ll \rho \ll \lambda_\parallel$, and

$$F_\rho(\rho) = -\frac{\phi_0^2}{4\pi^2N^2\Lambda_D\rho}, \quad \rho \gg \Lambda_D. \tag{89}$$

For the special case of two layers ($N = 2$) and a separation $\rho \gg \Lambda_D$, the magnitude of the attractive force exerted by a pancake vortex in one layer upon a pancake vortex in the other layer [Eq. (89)] is equal to the magnitude of the repulsive force between two pancake vortices in the same layer [Eq. (86) with $\Lambda_s = N\Lambda_D$].

The energy per unit length of a uniformly tilted infinite stack of pancake vortices in an infinite stack of superconducting layers was calculated in Ref. [7]. The corresponding line tension $T(\theta)$ was calculated in Ref. [58] as a function of the angle θ relative to the z axis and found to be positive only for $\theta < 51.8°$, indicating an instability beginning at 51.8°. Further calculations [58] showed that, because pancake vortices energetically prefer to line up parallel to the z axis, the energy for an infinite stack of pancake vortices with a large average tilt angle is reduced when the stack breaks up into shorter stacks parallel to the z axis with kinks between them. Pe *et al*. [59] calculated the equilibrium positions of a stack of pancake vortices in a finite stack of Josephson-decoupled layers when equal and opposite transport currents are applied to the top and bottom layers. They found that the pancake vortices in the top and bottom layers have large displacements to the left and right, while the other vortices all remain close to the z axis. Related model calculations were carried out in Ref. [60] for moving two-dimensional pancake vortex lattices in a finite stack of magnetically coupled superconducting thin films with transport current only in the top layer. For small currents, the entire electromagnetically coupled vortex array moves uniformly in the direction of the Lorentz force but with a large displacement of the pancake vortices in the top layer relative to the others, which remain in nearly straight lines perpendicular to the layers. Above a critical decoupling current, the 2D vortex array in the top layer periodically slips relative to the arrays in the other layers, and the dc current–voltage characteristics for

the top and bottom layers resemble those reported in Refs. [45] and [46] for the dc transformer.

6. JOSEPHSON COUPLING

The equations underlying the solutions presented in Secs. 2, 3, and 4 assume no interlayer Josephson coupling. Implicit in these solutions is the assumption that the component of the magnetic field parallel to the layers spreads out uniformly in the radial direction. This is consistent with the idea that if a magnetic field is applied parallel to a stack of Josephson-decoupled layers, the field will penetrate uniformly between the layers.

When the layers are Josephson-coupled, however, parallel magnetic fields penetrate the structure in the form of quantized Josephson vortices [61,62]. As discussed in Ref. [62], Josephson vortices in the high-temperature superconductors have highly elliptical current and field patterns. Since the decay length for currents perpendicular to the layers is λ_c and that for currents parallel to the layers is λ_{ab}, the ratio of the width of the pattern parallel to the layers to the height perpendicular to the layers is $\gamma = \lambda_c/\lambda_{ab}$ at large distances from the nonlinear Josephson core. For a high-κ Abrikosov vortex [49] in an isotropic superconductor, the decay length at large distances is the penetration depth λ, and the currents in the nonlinear core vary on the much smaller length scale of the coherence length ξ. The behavior in a Josephson vortex is analogous. The small length scale for spatial variation of the Josephson currents in the vortex core (whose axis is centered in the insulating layer between two adjacent superconducting layers) is the Josephson length [62,63] $\lambda_J = \gamma s$, while the corresponding length scale for the return of these currents parallel to the layers is s, such that the ratio of the width to the height of the Josephson core is $\gamma = \lambda_J/s = \lambda_c/\lambda_{ab}$.

In the presence of interlayer Josephson coupling, the magnetic-field and current-density distributions generated by a pancake vortex are unaltered at short distances but are strongly affected at distances of the order of λ_J and λ_c. To give an example, imagine an infinite stack of semi-infinite Josephson-coupled superconducting layers, all parallel to the xy plane, filling the half-space $x > 0$, such that the surface coincides with the plane $x = 0$. Imagine creating a pancake vortex at the origin in the superconducting layer $n = 0$ and moving it in to a distance x_0. The magnetic-field and current-density distributions, including the effects of a dipole-like stray field that leaks out into the space $x < 0$, have been calculated as a function of x_0 in Ref. [64] under the assumption of very weak Josephson coupling. In the presence of Josephson coupling, however, the component of the magnetic field parallel to the layers cannot penetrate with a power-law dependence to large distances but rather must decay exponentially with the decay length λ_c, because this component of the field induces Josephson currents to flow perpendicular to the layers. As the pancake vortex moves deeper into the stack, the Josephson coupling begins to play a greater role. When the pancake vortex is a distance λ_J or greater from the surface, a Josephson core region of width $2\lambda_J$ appears in the region between the vortex axis and the surface. Finally, at distances such that $x_0 \gg \lambda_c$, the current and field distribution can be characterized as a pancake vortex in which the fields at distances less than λ_J from the axis are nearly the same as in the Josephson-decoupled case, and the magnetic flux carried up through the pancake layer $z = 0$ is $\phi_0\,(s/2\lambda_\parallel)$. However, this magnetic flux does not flow radially outward to infinity as in the Josephson-decoupled case but instead is confined within a highly elliptical field distribution consisting of an overlapping Josephson vortex–antivortex pair, which links the pancake vortex to the surface. Recall that when a straight vortex is at a distance x from the surface of an isotropic superconductor of penetration depth λ, the magnetic flux inside the superconductor, calculated accounting for the image vortex at $-x$, is $\phi_0[1 - \exp(-x/\lambda)]$. As a pancake vortex moves from the surface to a position x_0 deep within the superconductor, it drags along a Josephson vortex (carrying magnetic flux in the $+x$ direction) whose axis is in the insulating layer at $z = -s/2$, and it also drags along a Josephson antivortex (carrying magnetic flux in the $-x$ direction) whose axis is in the insulating layer at $z = +s/2$. Accounting for the overlapping field distributions, which nearly cancel each other, we find that the magnetic flux carried in the $+x$ direction through the space $z < 0$ is $\phi_0[1 - \exp(-s/2\lambda_\parallel)] \approx \phi_0(s/2\lambda_\parallel)$; the same amount of magnetic flux is carried back in the $-x$ direction through the space $z > 0$.

To give another example, consider an infinite stack of pancake vortices initially aligned along the z axis in an infinite stack of Josephson-decoupled superconducting layers. As discussed at the end of Sec. 2, the field and current distributions reduce to those of a line vortex in an isotropic superconductor of penetration depth $\lambda_\parallel$ [48]. The magnetic field is

everywhere perpendicular to the layers. Now imagine displacing all of the pancake vortices in the space $z > s/2$ by a distance x_0 in the x direction, such that the pancake vortex stack now has a kink at $z = s/2$. In the absence of Josephson coupling, the resulting field and current distributions can be obtained by superposing those given in Sec. 2. A component of the field parallel to the layers must arise in order to displace the magnetic flux ϕ_0 whose distribution is centered on the z axis for $z \ll -\lambda_\parallel$ to a distribution centered on the line $(x, y) = (x_0, 0)$ for $z \gg \lambda_\parallel$. The component of the field parallel to the layers has a dipole-like distribution in any plane $z = \text{const}$, with a power-law dependence at large distances, but it decreases exponentially for $|z| > \lambda_\parallel$ because of the screening currents that flow parallel to the layers. In the presence of interlayer Josephson coupling, the above picture is altered, and it is now useful to think of kinked vortices as stacks of pancake vortices connected by Josephson strings (short pieces of Josephson vortices). The axes of the Josephson strings are confined to the insulating regions between superconducting layers. As a consequence of the Josephson coupling, the radial component of the magnetic field is screened on the length scale of λ_c by the induced Josephson currents, which flow perpendicular to the layers. Although there is little perturbation of the original field distribution when $x_0 < \lambda_J$, the Josephson length, this situation is altered when $x_0 > \lambda_J$, because in this case a nonlinear Josephson core appears along the string connecting the two pancake vortices centered at $(x, y, z) = (0, 0, 0)$ and $(x, y, z) = (x_0, 0, s)$. The Josephson-energy cost of the Josephson string coupling the two semi-infinite stacks of pancake vortices is approximately (taking logarithmic terms to be of order unity) [11,63,65–68]

$$E_{\text{short}}(x_0) \approx (\phi_0/4\pi)^2 x_0^2/s\lambda_c^2, \quad x_0 < \lambda_J = (\lambda_c/\lambda_{ab})s, \tag{90}$$

when the Josephson string is short and its core is not fully formed. The Josephson-energy cost is of the order of [11,61–63,65–69]

$$E_{\text{long}}(x_0) \approx (\phi_0/4\pi)^2 x_0/\lambda_{ab}\lambda_c, \quad x_0 > \lambda_J = (\lambda_c/\lambda_{ab})s, \tag{91}$$

when the Josephson string is long and its core is more fully formed. However, it is not until $x_0 \gg \lambda_c$ that a fully formed Josephson vortex (with width $2\lambda_c$ and height $2\lambda_{ab}$) can stretch out between the upper and lower parts of the split stack of pancake vortices. In this case the energy cost of the Josephson string coupling the two semi-infinite stacks of pancake vortices reduces to $(\phi_0 H_{c1,ab}/4\pi)x_0$, where $\phi_0 H_{c1,ab}/4\pi$ is the energy per unit length of an isolated Josephson vortex parallel to the layers [61,67,69,70] and

$$H_{c1,ab} = \frac{\phi_0}{4\pi\lambda_{ab}\lambda_c}\left[\ln\left(\frac{\lambda_{ab}}{s}\right) + 1.55\right]. \tag{92}$$

is the lower critical field parallel to the layers.

In anisotropic superconductors consisting of Josephson-coupled superconducting layers, one may always regard the vortex structure as consisting of a superposition of 2D pancake vortices, which carry magnetic flux up through the layers, and Josephson vortices (or strings), which carry magnetic flux parallel to the layers but no net flux perpendicular to the layers. In transport experiments involving vortex motion, the voltages are given by the Josephson relations [31]. The dc voltage parallel to the layers is $V_\parallel = (h/2e)\nu_\parallel$, where $\nu_\parallel$ is the time-averaged rate with which 2D pancake vortices cross a line between the contacts, and the dc voltage perpendicular to the layers is proportional to $V_\perp = (h/2e)\nu_\perp$, where $\nu_\perp$ is the time-averaged rate with which the axes of Josephson vortices (or strings) cross a line between the contacts.

When the Josephson coupling is strong, vortex lines tilted with respect to the z (or c) axis can be described as tilted stacks of 2D pancake vortices or as a tilted lattice, where pancakes in adjacent layers are connected by Josephson strings. Such vortices, sometimes called kinked vortex lines [71,72] have been studied by numerous authors [70,73–76] However, when the Josephson coupling is very weak, a magnetic field applied at a small angle relative to the layers can produce a structure consisting of two perpendicular interpenetrating lattices [63,77,78] (called a combined lattice [63] or crossing lattices [78]): a lattice of pancake vortices aligned nearly perpendicular to the layers and a lattice of Josephson vortices parallel to the layers. The interaction between the two kinds of vortices leads to striking chain-like vortex patterns in highly anisotropic Bi-2212, which have been observed by Bitter decoration [79,80] and scanning Hall-probe microscopy [35,81,82]. Both techniques reveal the positions of 2D pancake vortices within about λ_{ab} of the surface. As shown by Koshelev [83], in highly anisotropic layered superconductors the interactions between pancake vortices and Josephson vortices lead to deformations of both the pancake-vortex and Josephson-vortex crystals and to pinning of Josephson vortices by pancake vortices.

At high temperatures and applied magnetic fields, the vortex lattice melts [84–88], and this process has even been directly visualized in Bi-2212 by scanning Hall-probe microscopy [89,90]. The authors of Ref. [90] used the formalism of Sec. 4.1 A to infer the Lindemann parameter from the rms thermal fluctuations of pancake vortices versus magnetic field just below the melting transition. Much experimental and theoretical research has been devoted to vortex-lattice melting, and the reader is referred to reviews by Blatter *et al.* [91] and Brandt [92] for a more complete discussion of this topic.

The pinning of vortices by point defects is another topic where the interactions between pancake vortices and Josephson vortices play a key role. This difficult subject is further complicated by the effects of thermal fluctuations, especially in the high-temperature superconductors at the elevated temperatures where potential applications are most interesting. The reader is referred to the above reviews [91,92] and the recent paper by Kierfeld [93] for further details about this subject.

7. SUMMARY

In this paper, I have presented solutions that permit the calculation of the magnetic-field and current-density distributions generated by a single 2D pancake vortex in an infinite stack (Sec. 2), semi-infinite stack (Sec. 3), or a finite-thickness stack (Sec. 4) of Josephson-decoupled superconducting layers. I have shown in Sec. 5 how to calculate the electromagnetic forces between two pancake vortices, and in Sec. 6, I have discussed some of the ways that interlayer Josephson coupling modifies the results.

The results of this paper should be useful to those using probes (such as scanning Hall-probe microscopy, scanning SQUID microscopy, Bitter decoration, and magneto-optics) of the vortex-generated magnetic-field distributions above anisotropic high-temperature superconductors. If the sample surface is parallel to the cuprate planes, these probes measure chiefly the magnetic fields generated by pancake vortices within about λ_{ab} of the top surface. Although Josephson vortices (or strings) produce no net magnetic flux through the top surface, they can produce dipole-like stray fields if they are within λ_{ab} of the surface. On the other hand, if the sample surface is normal to the cuprate planes, such probes measure chiefly the magnetic fields generated by Josephson vortices within about λ_c of the sample surface, although pancake vortices within λ_{ab} of the surface can produce dipole-like stray fields outside the sample [64].

The pancake-vortex field and current distributions given in Secs. 2–4 also could be useful in analyzing experiments such as Lorentz microscopy [94–100] that probe the magnetic-field distribution throughout the sample thickness.

Since the London model is at the heart of the above pancake-vortex calculations, the resulting theoretical field and current distributions have unphysical singularities at the pancake-vortex core, which is of size $\sim\xi_{ab}$. Such singularities should have no experimental consequences for the above probes, which have insufficient resolution to reveal details at this length scale. However, for probes of higher resolution it may be necessary to take into account the fact that the circulating current density reaches a maximum at $\rho \approx \xi_{ab}$, and vanishes linearly as $\rho \to 0$, such that the singularity of the magnetic field at the pancake-vortex core is removed. The core effects could be treated approximately by using a vortex-core model that employs a variational core-radius parameter $\xi_v \sim \xi_{ab}$, as in Refs. [37,50–52].

APPENDIX: INTEGRALS USEFUL FOR $D \ll \lambda_\parallel$

Several integrals appear in Sec. 4.2. All may be evaluated by starting from [101,102]

$$\int_0^\infty du \frac{J_0(zu)}{1+u} = \frac{\pi}{2}\left[\boldsymbol{H}_0(z) - Y_0(z)\right], \tag{A.1}$$

where $\boldsymbol{H}_n(z)$ is the Struve function and $Y_n(z)$ is the Bessel function of the second kind (Weber's function), differentiating with respect to z, making use of recurrence relations, integrating by parts, and making use of the properties that [101,102]

$$\int_0^\infty du J_0(zu) = \int_0^\infty du J_1(zu) = \frac{1}{z}, \tag{A.2}$$

$$\int_0^\infty du \frac{J_1(zu)}{u} = 1. \tag{A.3}$$

The vector potential $a_\phi(\rho, 0)$ is proportional to

$$\int_0^\infty du \frac{J_1(zu)}{1+u} = \frac{1}{z} + 1 - \frac{\pi}{2}\left[\boldsymbol{H}_1(z) - Y_1(z)\right] \tag{A.4}$$

$$\approx 1, z \ll 1, \tag{A.5}$$

$$\approx \frac{1}{z}, z \gg 1, \quad \text{(A.6)}$$

where the limiting forms for $z \ll 1$ and $z \gg 1$ are obtained from expansions given in Refs. [101] and [102]. However, Eq. (A.5) may be obtained more simply by noting that, because of the properties of $J_1(uz)$, the integral when $z \ll 1$ is dominated by values of $u \gg 1$, such that $1 + u$ may be replaced by u; the resulting integral then takes the form of Eq. (A.3). Similarly, Eq. (A.6) may be obtained by noting that when $z \gg 1$ the integral is dominated by values of $u \ll 1$, such that $1 + u$ may be replaced by 1; the resulting integral may be evaluated using Eq. (A.2). The limiting forms of the following integrals also may be obtained in a similar fashion.

The magnetic field component $b_z(\rho, 0)$ is proportional to

$$\int_0^\infty du \frac{uJ_0(zu)}{1+u} = \frac{1}{z}\int_0^\infty du \frac{uJ_1(zu)}{(1+u)^2} = \frac{1}{z^2}\int_0^\infty du \frac{(1-u)J_0(zu)}{(1+u)^3} \quad \text{(A.7)}$$

$$= \frac{1}{z} - \frac{\pi}{2}[\boldsymbol{H}_0(z) - Y_0(z)] \quad \text{(A.8)}$$

$$\approx \frac{1}{z}, \quad z \ll 1, \quad \text{(A.9)}$$

$$\approx \frac{1}{z^3}, \quad z \gg 1, \quad \text{(A.10)}$$

and the net sheet current $K_D(\rho)$ is proportional to

$$\int_0^\infty du \frac{uJ_1(zu)}{1+u} = \frac{1}{z}\int_0^\infty du \frac{J_0(zu)}{(1+u)^2} \quad \text{(A.11)}$$

$$= \frac{\pi}{2}[\boldsymbol{H}_1(z) - Y_1(z)] \quad \text{(A.12)}$$

$$\approx \frac{1}{z}, \quad z \ll 1, \quad \text{(A.13)}$$

$$\approx \frac{1}{z^2}, \quad z \gg 1. \quad \text{(A.14)}$$

ACKNOWLEDGMENTS

I thank S. J. Bending, P. G. Clem, J. W. Guikema, J. Hoffman, and V. G. Kogan for stimulating discussions and correspondence. This article has been authored in part by Iowa State University of Science and Technology under Contract No. W-7405-ENG-82 with the U.S. Department of Energy.

REFERENCES

1. J. Bardeen, L. N. Cooper, and J. R. Schrieffer, *Phys. Rev.* **108,** 1175 (1957).
2. J. R. Clem, *Phys. Rev.* **148,** 392 (1966).
3. J. R. Clem, *Ann. Phys. (N.Y.)* **40,** 268 (1966).
4. D. M. Ginsberg, P. L. Richards, and M. Tinkham, *Phys. Rev. Lett.* **3**, 337 (1959).
5. M. Tinkham, *Introduction to Superconductivity* (McGraw-Hill, New York, 1975).
6. M. Tinkham, *Introduction to Superconductivity,* 2nd edn. (McGraw-Hill, New York, 1996).
7. J. R. Clem, *Phys. Rev. B* **43,** 7837 (1991).
8. S. N. Artemenko and A. N. Kruglov, *Phys. Lett. A* **143,** 485 (1990).
9. A. Buzdin and D. Feinberg, *J. Phys. (Paris)* **51,** 1971 (1990).
10. K. B. Efetov, *Sov. Phys. JETP* **49,** 905 (1979).
11. R. G. Mints, V. G. Kogan, and J. R. Clem, *Phys. Rev. B* **61,** 1623 (2000).
12. J. R. Clem, *Physica C* **235–240,** 2607 (1994).
13. J. Pearl, *Appl. Phys. Lett.* **5,** 65 (1964).
14. J. Pearl, in *Proceedings of the Ninth International Conference on Low Temperature Physics*, J. G. Daunt, D. V. Edwards, F. J. Milford, and M. Yaqub, eds. (Plenum, New York, 1965), Part A, p. 566.
15. P. G. de Gennes, *Superconductivity of Metals and Alloys* (Benjamin, New York, 1966), p. 60.
16. M. von Laue, *Theory of Superconductivity* (Academic Press, New York, 1952).
17. C. Caroli, P. G. de Gennes, and J. Matricon, *J. Phys. Kondens. Mater.* **1,** 176 (1963).
18. L. P. Gor'kov and T. K. Melik-Barkhudarov, *Sov. Phys. JETP* **18,** 1031 (1964).
19. D. R. Tilley, G. J. Van Gurp, and C. W. Berghout, *Phys. Lett.* **12,** 305 (1964).
20. D. R. Tilley, *Proc. Phys. Soc. Lond.* **85,** 1977 (1965); **86,** 289 (1965).
21. E. I. Katz, *Sov. Phys. JETP* **29,** 897 (1969).
22. E. I. Katz, *Sov. Phys. JETP* **31,** 787 (1970).
23. K. Takanaka, *Phys. Status Solidi B* **68,** 623 (1975).
24. R. A. Klemm and J. R. Clem, *Phys. Rev. B* **21,** 1868 (1980).
25. V. G. Kogan, *Phys. Rev. B* **24,** 1572 (1981).
26. V. G. Kogan and J. R. Clem, *Phys. Rev. B* **24,** 2497 (1981).
27. V. G. Kogan and J. R. Clem, *Jpn. J. Appl. Phys.* **26** (Suppl. 26–3), 1159 (1987).
28. A. V. Balatskii, L. I. Burlachkov, and L. P. Gor'kov, *Sov. Phys. JETP* **63,** 866 (1986).
29. L. N. Bulaevskii, V. L. Ginzburg, and A. Sobyanin, *Sov. Phys. JETP* **68,** 1499 (1988).
30. W. E. Lawrence and S. Doniach, in *Proceedings of the Twelfth International Conference on Low Temperature Physics,* E. Kanda, ed. (Academic Press of Japan, Kyoto, 1971), p. 361.
31. B. D. Josephson, *Phys. Lett.* **1,** 251 (1962).
32. J. R. Clem, *Physica C* **162–164,** 1137 (1989).
33. P. H. Kes, J. Aarts, V. M. Vinokur, and C. J. van der Beek, *Phys. Rev. Lett.* **64,** 1063 (1990).
34. J. C. Martínez, S. H. Brongersma, A. Koshelev, B. Ivlev, P. H. Kes, R. P. Griessen, D. G. de Groot, Z. Tarnavski, and A. A. Menovsky, *Phys. Rev. Lett.* **69,** 2276 (1992).
35. A. N. Grigorenko, S. J. Bending, A. E. Koshelev, J. R. Clem, T. Tamegai, and S. Ooi, *Phys. Rev. Lett.* **89,** 217003 (2002).
36. J. R. Clem, *Phys. Rev. B* **9,** 898 (1974).
37. J. R. Clem, *Phys. Rev. B* **12,** 1742 (1975).
38. I. Giaever, *Phys. Rev. Lett.* **15,** 825 (1965).
39. I. Giaever, *Phys. Rev. Lett.* **16,** 460 (1966).
40. P. R. Solomon, *Phys. Rev. Lett.* **16,** 50 (1966).
41. M. D. Sherrill, *Phys. Lett. A* **24,** 312 (1967).
42. R. Deltour and M. Tinkham, *Phys. Rev.* **174,** 478 (1968).

43. P. E. Cladis, *Phys. Rev. Lett.* **21,** 1238 (1968).
44. P. E. Cladis, R. D. Parks, and J. M. Daniels, *Phys. Rev. Lett.* **21,** 1521 (1968).
45. J. W. Ekin, B. Serin, and J. R. Clem, *Phys. Rev. B* **9,** 912 (1974).
46. J. W. Ekin and J. R. Clem, *Phys. Rev. B* **12,** 1753 (1975).
47. F. London, *Superfluids*, Vol. 1 (Dover, New York, 1961).
48. M. Tinkham, *Introduction to Superconductivity,* 2nd edn. (McGraw-Hill, New York, 1996) p. 152.
49. A. A. Abrikosov, *Sov. Phys. JETP* **5,** 1174 (1957).
50. J. R. Clem, *J. Low Temp. Phys.* **18,** 427 (1975).
51. J. R. Clem, Z. Hao, L. Dobrosavljević-Grujić, and Z. Radović, *J. Low Temp. Phys.* **88,** 213 (1992). On p. 216 of this paper, the number 0.479 should be corrected to 0.497.
52. J. R. Clem, in *Inhomogeneous Superconductors—1979*, D. U. Gubser, T. L. Francavilla, S. A. Wolf, and J. R. Leibowitz, eds. (American Institute of Physics, New York, 1980), p. 245.
53. J. Pearl, *J. Appl. Phys.* **37,** 4139 (1966).
54. J. D. Jackson, *Classical Electrodynamics* (Wiley, New York, 1962), p. 77.
55. J. R. Clem, *Phys. Rev. B* **5,** 2140 (1970). The prefactor on the right-hand side of Eq. (3.11) of this paper should be corrected to $(\phi_0/4\pi\lambda^2)$.
56. J. W. Guikema, PhD dissertation, Stanford University, March 2004.
57. M. Tinkham, *Introduction to Superconductivity,* 2nd edn. (McGraw-Hill, New York, 1996), p. 155.
58. M. Benkraouda and J. R. Clem, *Phys. Rev. B* **53,** 438 (1996).
59. T. Pe, M. Benkraouda, and J. R. Clem, *Phys. Rev. B* **55,** 6636 (1997).
60. T. Pe, M. Benkraouda, and J. R. Clem, *Phys. Rev. B* **56,** 8289 (1997).
61. L. N. Bulaevskii, *Sov. Phys. JETP* **37,** 1133 (1973).
62. J. R. Clem and M. W. Coffey, *Phys. Rev. B* **42,** 6209 (1990).
63. L. N. Bulaevskii, M. Ledvij, and V. G. Kogan, *Phys. Rev. B* **46,** 355 (1992).
64. R. G. Mints, I. B. Snapiro, and E. H. Brandt, *Phys. Rev. B* **54,** 9458 (1996).
65. L. I. Glazman and A. E. Koshelev, *Physica C* **173,** 180 (1991).
66. A. Kapitulnik, in *Phenomenology and Applications of High-Temperature Superconductors*, K. S. Bedell, M. Inui, D. Meltzer, J. R. Schrieffer, and S. Doniach, eds. (Addison-Wesley, Reading, 1992), p. 34.
67. L. N. Bulaevskii, M. Ledvij, and V. G. Kogan, *Phys. Rev. B* **46,** 11807 (1992).
68. J. R. Clem, *Physica A* **200,** 118 (1993).
69. J. R. Clem, M. W. Coffey, and Z. Hao, *Phys. Rev. B* **44,** 2732 (1991).
70. A. E. Koshelev, *Phys. Rev. B* **48,** 1180 (1993) and private communication.
71. D. Feinberg and C. Villard, *Mod. Phys. Lett.* **4,** 9 (1990).
72. D. Feinberg and C. Villard, *Phys. Rev. Lett.* **65,** 919 (1990).
73. B. I. Ivlev, Y. N. Ovchinnikov, and V. L. Pokrovskii, *Mod. Phys. Lett.* **5,** 9 (1990).
74. S. S. Maslov and V. L. Pokrovskii, *Europhys. Lett.* **14,** 591 (1991).
75. S. S. Maslov and V. L. Pokrovskii, *JETP Lett.* **53,** 637 (1991).
76. D. Feinberg, *Physica C* **194,** 126 (1992).
77. D. A. Huse, *Phys. Rev. B* **46,** 8621 (1992).
78. A. E. Koshelev, *Phys. Rev. Lett.* **83,** 189 (1999).
79. C. A. Bolle, P. L. Gammel, D. J. Bishop, D. Mitzi, and A. Kapitulnik, *Phys. Rev. Lett.* **68,** 3343 (1991).
80. I. V. Grigorieva, J. W. Steeds, G. Balakrishnan, and D. M. Paul, *Phys. Rev. B* **51,** 3765 (1995).
81. A. Oral, S. J. Bending, and M. Henini, *Appl. Phys. Lett.* **69,** 1324 (1996).
82. A. N. Grigorenko, S. J. Bending, T. Tamegai, S. Ooi, and M. Henini, *Nature (London)* **414,** 728 (2001).
83. A. E. Koshelev, *Phys. Rev. B* **68,** 094520 (2003).
84. H. Safar, P. L. Gammel, D. A. Huse, D. J. Bishop, J. P. Rice, and D. M. Ginsberg, *Phys. Rev. Lett.* **69,** 824 (1992).
85. W. K. Kwok, S. Fleshler, U. Welp, V. M. Vinokur, J. Downey, G. W. Crabtree, and M. M. Miller, *Phys. Rev. Lett.* **69,** 3370 (1992).
86. R. Cubitt, E. M. Forgan, G. Yang, S. L. Lee, D. M. Paul, H. M. Mook, M. Yethiraj, P. H. Kes, T. W. Li, A. A. Menovsky, Z. Tarnavski, and K. Mortensen, *Nature (London)* **365,** 407 (1993).
87. E. Zeldov, D. Majer, M. Konczykowski, V. B. Geshkenbein, V. M. Vinokur, and H. Shtrikman, *Nature (London)* **375,** 373 (1995).
88. A. Schilling, R. A. Fisher, N. E. Phillips, U. Welp, D. Dasgupta, W. K. Kwok, and G. W. Crabtree, *Nature (London)* **382,** 791 (1996).
89. A. Oral, J. C. Barnard, S. J. Bending, I. I. Kaya, S. Ooi, T. Tamegai, and M. Henini, *Phys.Rev. Lett.* **80,** 3610 (1998).
90. S. J. Bending, A. Oral, J. R. Clem, I. I. Kaya, S. Ooi, T. Tamegai, and M. Henini, *IEEE Trans. Appl. Supercond.* **9,** 1820 (1999).
91. G. Blatter, M. V. Feigelman, V. B. Geshkenbein, A. I. Larkin, and V. M. Vinokur, *Rev. Mod. Phys.* **66,** 1125 (1994).
92. E. H. Brandt, *Rep. Prog. Phys.* **58,** 1465 (1995).
93. J. Kierfeld, *Phys. Rev. B* **69,** 144513 (2004).
94. S. Fanesi, G. Pozzi, J. E. Bonevich, O. Kamimura, H. Kasai, K. Harada, T. Matsuda, and A. Tonomura, *Phys. Rev. B* **59,** 1426 (1999).
95. T. Yoshida, J. Endo, K. Harada, H. Kasai, T. Matsuda, O. Kamimura, A. Tonomura, M. Beleggia, R. Patti, and G. Pozzi, *J. Appl. Phys.* **85,** 4096 (1999).
96. T. Matsuda, O. Kamimura, H. Kasai, K. Harada, T. Yoshida, T. Akashi, A. Tonomura, Y. Nakayama, J. Shimoyama, K. Kishio, T. Hanaguri, and K. Kitazawa, *Science* **294,** 2136 (2001).
97. O. Kamimura, H. Kasai, T. Akashi, T. Matsuda, K. Harada, J. Masuko, T. Yoshida, N. Osakabe, A. Tonomura, M. Beleggia, G. Pozzi, J. Shimoyama, K. Kishio, T. Hanaguri, K. Kitazawa, M. Sasase, and S. Okayasu, *J. Phys. Soc. Jpn.* **71,** 1840 (2002).
98. M. Beleggia, G. Pozzi, J. Masuko, K. Harada, T. Yoshida, O. Kamimura, H. Kasai, T. Matsuda, and A. Tonomura, *Phys. Rev. B* **66,** 174518 (2002).
99. A. Tonomura, *Physica C* **388–389,** 624 (2003).
100. A. Tonomura, *J. Low Temp. Phys.* **131,** 941 (2003).
101. I. S. Gradshteyn and I. M. Ryzhik, *Table of Integrals, Series, and Products*, 6th edn. (Academic Press, San Diego, 2000).
102. M. Abramowitz and I. A. Stegun, eds., *Handbook of Mathematical Functions* (National Bureau of Standards, Washington, 1967).